Lab on a Chip

RSC Publishing

PAPER

View Article Online
View Journal | View Issue

Cite this: *Lab Chip*, 2013, **13**, 1883

Side view thrombosis microfluidic device with controllable wall shear rate and transthrombus pressure gradient†

Ryan W. Muthard and Scott L. Diamond*

Hemodynamic conditions vary throughout the vasculature, creating diverse environments in which platelets must respond. To stop bleeding, a growing platelet deposit must be assembled in the presence of fluid wall shear stress (τ_w) and a transthrombus pressure gradient (ΔP) that drives bleeding. We designed a microfluidic device capable of pulsing a fluorescent solute through a developing thrombus forming on collagen ± tissue factor (TF), while independently controlling ΔP and τ_w. Computer control allowed step changes in ΔP with a rapid response time of 0.26 mm Hg s^{-1} at either venous (5.2 dynes cm^{-2}) or arterial (33.9 dynes cm^{-2}) wall shear stresses. Side view visualization of thrombosis with transthrombus permeation allowed for quantification of clot structure, height, and composition at various ΔP. Clot height was reduced 20% on collagen/TF and 28% on collagen alone when ΔP was increased from 20.8 to 23.4 mm Hg at constant arterial shear stress. When visualized with a platelet-targeting thrombin sensor, intrathrombus thrombin levels decreased by 62% as ΔP was increased from 0 to 23.4 mm Hg across the thrombus-collagen/TF barrier, consistent with convective removal of thrombogenic solutes due to pressure-driven permeation. Independent of ΔP, the platelet deposit on collagen had a permeability of 5.45×10^{-14} cm^2, while the platelet/fibrin thrombus on collagen/TF had a permeability of 2.71×10^{-14} cm^2 (comparable to that of an intact endothelium). This microfluidic design allows investigation of the coupled processes of platelet deposition and thrombin/fibrin generation in the presence of controlled transthrombus permeation and wall shear stress.

Received 4th December 2012,
Accepted 8th March 2013

DOI: 10.1039/c3lc41332b

www.rsc.org/loc

Introduction

At the onset of vessel injury, collagen and the subendothelial matrix become exposed to flowing blood. Hemostasis is maintained by platelet adhesion and aggregation at the site of injury[1] along with thrombin production triggered by extravascular tissue factor molecules. The local physical and biological stimuli present during this development play a critical role in the final clot structure and function. One important physical parameter that has long been recognized is the prevailing wall shear stress (τ_w),[2] with the venous system having lower wall shear stresses than the arterial system.[3] Often absent in the design of *in vitro* models is the transthrombus pressure gradient (ΔP) that exists between the intraluminal space and the interstitial compartment of vascularized tissue. Incorporating this feature into thrombus development could quickly change the profile of soluble species, resulting in altered clot structures.

In recent years, several *in vivo* studies have demonstrated the importance of interstitial pressure and flow on angiogenesis.[4,5] This research has benefited from the ability to control physical factors, such as pressure gradients and shear rates using *in vitro* microfluidic devices. Previous work has illustrated a control of these parameters, but at levels not representative of the arterial vasculature.[6] Others have shown control of τ_w or ΔP, but decoupling their dependence at high and low shear stress is a difficult task.[7,8] Independently controlling both pressure gradients and wall shear stresses at arterial or venous conditions would provide an important understanding of hemostasis in blood vessel microenvironments. There have not been any devices that incorporate this level of control.

We were able to design and validate a microfluidic device capable of independently controlling the wall shear stress and *trans*-scaffold pressure gradient. Localization of collagen ± tissue factor (TF) in the scaffold region of the device allowed side view imaging of thrombosis under controlled transthrombus pressure drops. At arterial wall shear stress values, small increases in transthrombus pressure gradients significantly reduced the average platelet and platelet/fibrin clot heights. Similarly, the periphery and quantity of thrombin within the

Institute for Medicine and Engineering, Department of Chemical and Biomolecular Engineering, 1024 Vagelos Research Laboratory, University of Pennsylvania, Philadelphia, PA 19104 E-mail: sld@seas.upenn.edu; Tel: 215-573-5702

† Electronic supplementary information (ESI) available. See DOI: 10.1039/c3lc41332b

clot was reduced in the presence of increased transthrombus permeation. Permeability measurements were obtained under flow by utilizing dye pulsing. The collagen scaffold permeability was validated using previous literature values, and new measurements of platelet and platelet/fibrin clot permeability were calculated at various pressure drops. We demonstrate the ability to independently control *trans*-scaffold pressure gradients and wall shear stresses for studying the permeation effects and rates on or through thrombi.

Materials and methods

Device fabrication and design

Polydimethylsiloxane (PDMS) (Ellsworth Adhesives) microfluidic devices were fabricated using previously described soft lithography techniques.[9] In brief, photolithography was used to preferentially pattern negative photoresist (KMPR 1050, MicroChem Corp.) on a silicon wafer (D = 100 mm, WRS Materials). The photoresist was spun to a height of 60 μm then soft baked for 20 min. Following baking, the substrate was placed beneath a photomask and exposed to UV illumination. Prior to development (AZ® 300 MIF, AZ Electronic Materials USA Corp.), the substrate was baked for 4 min at 100 °C. PDMS, with a base to curing agent ratio of 10 : 1, was then molded on the substrate for 2 h at 80 °C. Inlet/outlet and pressure ports (Fig. 1A) were cut out using 0.75 and 0.5 mm I.D. corers (Harris Uni-Core™, Ted Pella, Inc.), respectively. PDMS-tubing (0.020″ ID × 0.060″ OD, Cole-Parmer) connections were made *via* 90°, 23 gauge × 1/2″ length blunt needles (Small Parts).

The device was designed with a primary channel (60 μm high × 250 μm wide) connected to two inlets (upstream, downstream), two outlets (scaffold, channel), and three pressure ports (P_1, P_2 and P_3). The upstream inlet was used for fluid that will come in direct contact with the scaffold, while the downstream inlet, prior to the compressed channel (200 μm wide), was added to create resistance to flow upstream (Fig. 1a). The added resistance caused increased pressure due to the constant volume of the syringe pumps. Two pressure ports were added upstream (P_2) and downstream (P_1) of the scaffold region to accurately measure the pressure at the scaffold–channel interface. An additional pressure port (P_3) was placed next to the scaffold outlet port to determine the pressure drop across the region. The scaffold was designed with an array of posts (D = 50 μm) spaced 20 μm apart with a narrowed opening from L = 250 μm at the interface to L = 50 μm at the exit (Fig. 1b). The posts positions were ideal for uniformly loading collagen fibers and the compressed exit forced the majority of the pressure drop across the scaffold rather than the exiting channel. Post arrays were placed surrounding each of the channel setups to support the negative pressure due to vacuum sealing to glass slides (Fig. 1c). All of the design features in this device made it possible to monitor and control the pressure gradients across the scaffold, while maintaining constant wall shear stress at the interface.

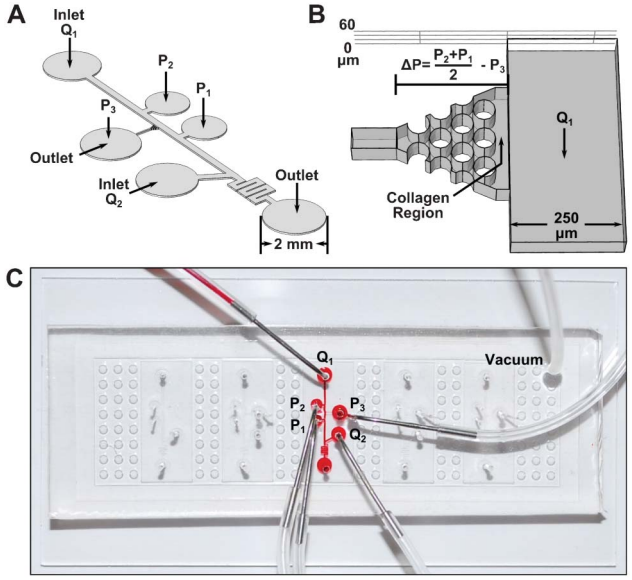

Fig. 1 A microfluidic device with controllable *trans*-scaffold pressure gradients. Syringe pump inlet Q_1 provided a constant volume flow that exited through the downstream outlet or transversed the collagen region towards the outlet monitored by P_3 (A). The main flow channel (H = 60 μm, W = 250 μm) provided a collagen–fluid flow interface between pressure sensors P_2 and P_1 (B). A LabVIEW control panel interpreted the pressure measurements (P_1, P_2 and P_3) and proportionately controlled a constant volume syringe pump (Q_2) to maintain constant pressure gradients across the collagen region. Prior to use, the PDMS microfluidic device was vacuum sealed to a glass slide and connections between the tubing and device were made *via* 90°, 23-gauge blunt needle tips (C).

Device operation

Devices were vacuum sealed to Sigmacote® (Sigma-Aldrich) treated glass slides and channels were coated with a 10% BSA solution for 30 min. Polymerized fibrillar collagen was prepared overnight by incubating (37 °C) an 8 : 1 : 1 ratio of collagen (3 mg ml^{-1} monomeric, human Type I) (Vitrocol, Advanced BioMatrix, Inc.), 10× PBS, and 0.09 M NaOH, respectively. Tissue factor liposomes were prepared as previously described.[10,11] Briefly, biotinylated anti-collagen (4 μg ml^{-1}, Abcam) and streptavidin (10 μg ml^{-1}, Sigma-Aldrich) were mixed subsequently in a 1 : 10 volumetric ratio with polymerized collagen. Following a 5 min incubation at room temperature for each, biotinylated/TF liposomes (79 : 20 : 1, L-α-phosphatidylcholine (PC): L-α-phosphatidylserine (PS): biotinylated phosphatidylethanolamine (bPE), Avanti Polar Lipids) were mixed in a 1 : 20 ratio by volume with the polymerized collagen/biotinylated anti-collagen/streptavidin mixture. The solution was incubated for an additional 10 min at room temperature. Device scaffolds were then loaded by pulling 2.5 μL of polymerized collagen (±TF liposomes) through pressure ports P_1 and P_2 out of the scaffold region exit. Immediately following loading, Ca^{2+} buffer (5 mM) was rinsed through the channels to remove any collagen outside of the scaffold. Devices were setup on a slide holder for imaging using a CCD camera (ORCA-ER, Hamamatsu) on an inverted microscope (IX81, Olympus America Inc.).

The loaded channel was then connected to the three pressure sensors (P_1, P_2 and P_3) and the upstream and downstream syringe pumps as previously discussed. The flow rate from the upstream pump (PHD Ultra, Harvard Apparatus) provided a constant initial wall shear stress (33.9 dyne cm^{-2}) at the scaffold by setting a constant flow rate (13 μl min^{-1}). Pressure transducers (Honeywell Sensing and Control) connected at the P_1, P_2 and P_3 ports transmitted analog voltage signals to a data acquisition device (NI USB-6210, National Instruments) that was used to process the measurements in LabVIEW (National Instruments, Fig. S1, ESI†). The flow rate from the downstream pump (PHD 2000, Harvard Apparatus) was controlled proportionately according to the real-time pressure measurements (Fig. S2 and S3, ESI†). This control allowed the device to maintain a constant pressure drop across the scaffold throughout the experiment.

Device validation

Pressure transducers were calibrated between 0–1 psig in LabVIEW using atmospheric pressure and 27.7 inches of H_2O. The device was validated by measuring the permeability of collagen loaded in the scaffold. An injection valve (V-450, IDEX Health & Science LLC) was placed between the syringe pump and the microfluidic channel (Q_1) to produce a controlled pulse under constant flow. The average velocity through the scaffold was measured by pulsing ~25 μL of sulforhodamine 101 acid chloride (Texas Red, Sigma-Aldrich) in 5 mM Ca^{2+} buffer through the channel and monitoring dye fluorescence intensity at the inlet and outlet of the collagen scaffold. Measuring the average velocity through the collagen allowed permeability to be calculated over the complex domain using COMSOL Multiphysics software. The resulting collagen permeability was validated by comparisons to previously determined literature values.[12,13] The permeability of platelet and platelet/fibrin deposited layers could then be measured using similar techniques by pulsing ~25 μL of fluorescein isothiocyanate (FITC, Sigma-Aldrich) in Ca^{2+} buffer (5 mM) following 10 min of whole blood flow (1130 s^{-1}) at a range of physiological pressure drops.[14,15]

Blood collection

Blood draws were in accordance with the University of Pennsylvania's IRB and all healthy volunteers were self reported as alcohol and medication free. Human blood was collected from donors directly into an anti-coagulant *via* venipuncture. Studies examining the absence of thrombin were completed with 100 μM of the anti-coagulant Phe-Pro-Arg-chloromethylketone (PPACK, Haematologic Technologies Inc.) and 1 μg ml^{-1} of a fluorescently conjugated anti-CD41 monoclonal antibody (Abd Serotec). Uninhibited thrombin studies were completed in 40 μg ml^{-1} of the anti-coagulant corn trypsin inhibitor (CTI, Haematologic Technologies Inc.) and 0.125 μg ml^{-1} of a PE-conjugated anti-CD61 antibody (Becton Dickinson Biosciences). CTI-treated blood was also supplemented with 5 μg ml^{-1} of a thrombin sensitive antibody (ThS-Ab) for thrombin localization studies,[16] 0.0625 μg ml^{-1} of a PE-conjugated anti-CD62P antibody (Becton Dickinson Biosciences) for P-selectin studies, and 0.5 μg ml^{-1} of a fluorescently conjugated anti-fibrin antibody (gift from the M. Poncz, Children's Hospital of Philadelphia) for fibrin localization studies.[17,18]

Finite element analysis

During the design phase of the microfluidic fabrication, COMSOL Multiphysics was used to predict the localization of collagen in the scaffold. The entire structure was modeled and the pressure ports were a source of collagen (C = 1), while the remainder of the ports with exception to the scaffold exit were a source of 5 mM Ca^{2+} (C = 0). The solution was pulled through the scaffold exit at a velocity (1 mL min^{-1}) similar to slowly pulling with a 1 mL syringe. Velocity profiles and concentration localization plots were used to predict the best suited scaffold design. COMSOL was also used to calculate clot wall shear stress on experimentally defined clot structures at two minute time intervals. Three-dimensional simulations were modeled using experimental clot structures in a 250 μm wide × 60 μm high channel. The inlet flow rate was set to 13 μL min^{-1} and the middle 60% of the clot surface was averaged over 100 equal spaced line scans for each time dependent structure. In an independent measurement, COMSOL was used to calculate permeability.[19] Briefly, the pulsed dye buffer was modeled using the stationary Navier–Stokes equation for laminar flow. The collagen, platelet deposit, and platelet/fibrin structures were simulated using Darcy's law:

$$\boldsymbol{u} = -\frac{\kappa}{\mu}\nabla p \quad (1)$$

where $\boldsymbol{u}$ is the fluid velocity, κ is the Darcy's permeability, μ is the buffer viscosity, and p is the pressure. Coupling the Navier–Stokes equation with eqn (1) allowed Darcy's permeability (κ) to be iteratively calculated by minimizing the squared error between the mean experimental and simulated fluid velocity through the porous media

Results

Controllable transcollagen scaffold ΔP in a side view thrombosis device

A microfluidic device was designed with the ability to maintain a computer-controlled *trans*-scaffold pressure gradient of $\Delta P = (P_2 - P_1)/2 - P_3$, while providing constant wall shear stress τ_w (Fig. 1). The pressure gradient and wall shear stress were controlled by utilizing two independent syringe pumps (Q_1, Q_2), three pressure sensors (P_1, P_2, P_3), and a proportional controller in LabVIEW (Fig. S1–S3, ESI†) to control Q_2 based on P_1, P_2, and P_3 at constant Q_1. The syringe pump upstream of the scaffold region dictated the wall shear stress, while the downstream syringe pump controlled the channel pressure for independent control of ΔP and τ_w.

The scaffold region was designed with six posts equally spaced in a triangular orientation (Fig. 1b and Fig. 2) to support the loading of fibrous matrix materials, such as polymerized collagen. Pressure ports upstream (P_2) and downstream (P_1) of the scaffold were used for even infusion of a collagen solution during the loading protocol by withdrawal from port P_3 (Fig. 2a). With Q_1 and Q_2 = 0, the velocity

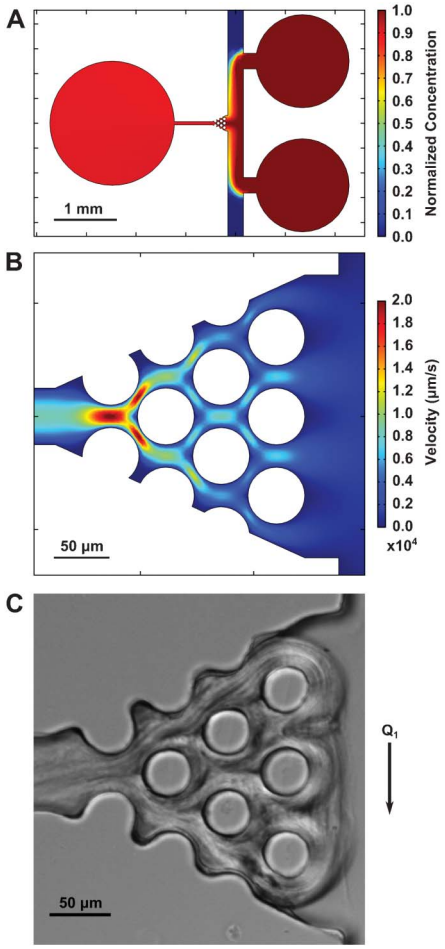

Fig. 2 Human type I, polymerized collagen localized in the scaffold region. Polymerized collagen (2.5 μL) was placed on pressure ports P_2 and P_1. A 1 mL syringe was used to pull the solution through the scaffold region allowing fibers to wrap around the posts. COMSOL simulations demonstrated the normalized concentration and the limited exposure of collagen in the channel during the loading procedure (A). The initial velocity field in the scaffold region produces slightly higher velocities in the middle of the posts, which allowed collagen fibers to load the middle of the region before the outer edges (B). This type of loading resulted in an evenly distributed collagen region with a flat collagen–fluid flow interface (C).

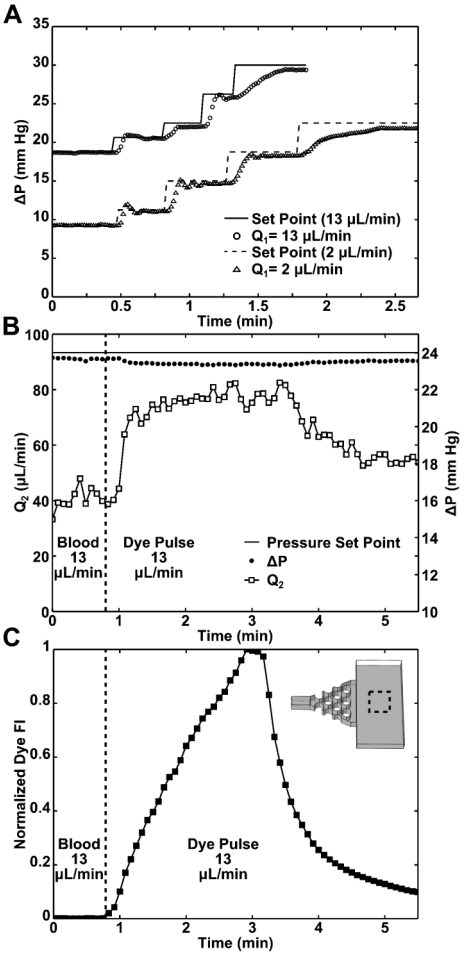

Fig. 3 Syringe pump control allows rapid responses to changes in pressure set point and fluid viscosity. Constant Q_1 flow rates provide a constant wall shear rate at the collagen–fluid flow interface. LabVIEW control over Q_2, *via* a downstream syringe pump, allowed pressure gradients across the scaffold region to remain constant, while responding quickly to set point adjustments (A). In a separate experiment, buffer containing dye was pulsed through the device. As the lower viscosity buffer became more concentrated than the blood, the Q_2 flow rate increased to maintain pressure at the desired set point (B). The increase in normalized dye fluorescence intensity corresponded to the decrease in viscosity and the increase in downstream flow rate Q_2 (C).

profile throughout the posts initially focuses collagen loading in the middle of the scaffold where the velocities are roughly twice as fast as the edges (Fig. 2b). As the middle region is loaded, the edge velocities start to dominate resulting in a uniform distribution of collagen at the interface of the main channel (Fig. 2c). This approach provided a reliable and repeatable method to create a defined protein matrix to trigger reactions during the subsequent perfusion of whole blood using Q_1.

After collagen was loaded into the device, the ΔP controller algorithm was optimized under diverse conditions. First, the proportionate control parameter K_p was determined to be 0.92 μL min^{-1} Pa using manual tuning to maximize the response speed and minimize overshoot. The maximum buffer flow rate was set to 100 μl min^{-1} to prevent overshooting the set point. Robust control of *trans*-scaffold ΔP set points was obtained under arterial (1130 s^{-1}, 13 μL min^{-1}) or venous (174 s^{-1}, 2 μL min^{-1}) wall shear rates (Fig. 3a) using whole blood perfusion. A range of ΔP values from 20.6 to 30 mm Hg were achieved at an arterial shear rate. Similarly, a range of ΔP values from 11.3 to 22.5 mm Hg were achieved at a venous shear rate. The average response rate was 0.26 mm Hg s^{-1} during set point changes. Lower wall shear stress required higher buffer flow rates to reach larger pressure gradients, which caused reduced response rates (0.20 mm Hg s^{-1}) compared to the arterial wall shear stress (0.31 mm Hg s^{-1}). Throughout these experiments P_2 and P_1 typically differed by less than 1 mm Hg, while P_3 remained relatively constant.

For measurement of clot permeability, pulsing of a fluorescent solute tracer under a constant flow rate was required. This feature was examined by measuring the *trans*-

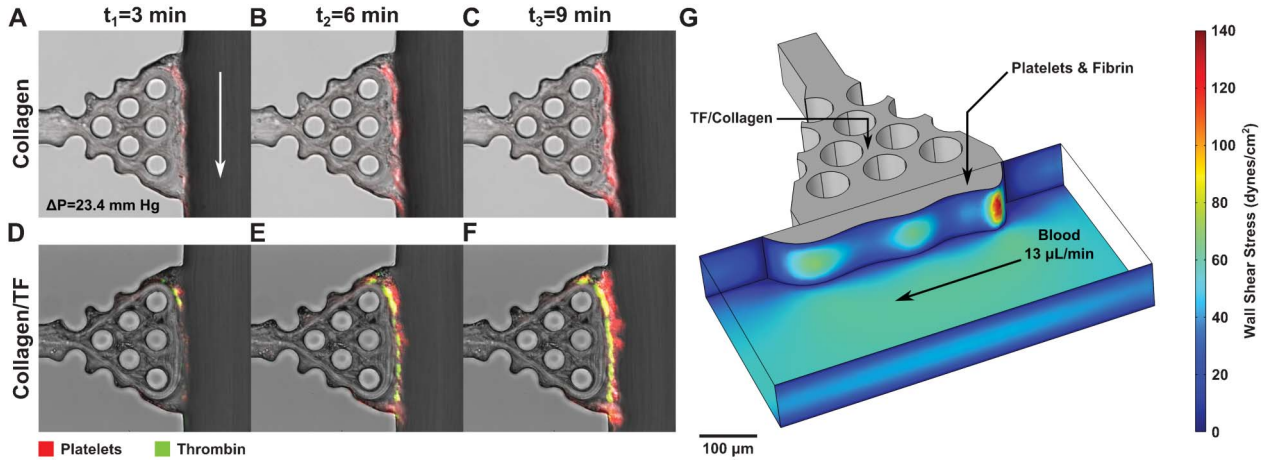

Fig. 4 Perfusion of anti-coagulated whole blood provides reproducible thrombus development at the collagen–blood interface. Anti-coagulated whole blood was perfused at an initial wall shear stress (33.9 dyne cm^{-2}), while a constant ΔP (23.4 mm Hg) was maintained across the collagen–blood interface. Dynamic studies of platelet (red) and thrombin (green) development on collagen (A–C) or collagen/TF scaffolds (D–F) allowed for spatial–temporal clot measurements. Resulting structures were simulated in COMSOL to study time-dependent wall shear stresses at the clot boundary (G).

scaffold pressure gradient and buffer flow rate during the injection of a fluorescent dye solution at a lower viscosity (μ_{Dye} = 0.001 Pa s) than that of whole blood (μ_{Blood} = 0.003 Pa s) (Fig. 3b).[20] Prior to the introduction of the dye (<1 min), the blood viscosity in the channel and the Q_2 flow rate were constant. As the dye in buffer solution began to exceed the blood concentration (1–3 min, Fig. 3c), the viscosity of the mixture began to drop. This drop in viscosity was met with an increase in the Q_2 flow rate to compensate for the reduction in resistance against the Q_1 syringe pump. When the blood began to exceed the dye–buffer solution (>3 min), the viscosity began to increase and the Q_2 flow rate began to decrease to provide a constant resistance against the Q_1 syringe pump. Throughout all of these viscosity changes the pressure drop in the channel remained constant (23.5 ± 0.12 mm Hg) due to the constant downstream resistance maintained by the Q_2 flow rate. The ΔP range that we investigated mimics the range located in capillaries. At the head or heart level lumen pressures are generally 25–30 mm Hg[14] and interstitial pressures are within −2–10 mm Hg.[15] While we have focused on this ΔP (15 mm Hg to 32 mm Hg), higher ΔP values certainly exist in physiology and can be achieved in this device.

Transthrombus permeation reduces the intrathrombus zone of thrombin activity

Thrombus development at the collagen or collagen/TF scaffold was followed for 10 min with a *trans*-scaffold pressure drop of 23.4 mm Hg. During the perfusion of PPACK anti-coagulated whole blood at an initial wall shear stress of 33.9 dyne cm^{-2}, the thrombin deficient clot formed a uniform layer at the collagen–blood interface (Fig. 4a–c). When TF was added to the collagen scaffold and PPACK was replaced with CTI, the clot favored larger upstream and downstream platelet deposits rather than the uniformity seen in thrombin deficient clots (Fig. 4d–f). Using a thrombin sensing anti-platelet antibody, we were able to clearly show the thrombin rich layer within the clot near the collagen/TF interface during transthrombus permeation. The clot structure was then modeled in COMSOL to analyze the resulting wall shear stress at the surface of the clot following 9 min of flow. Due to the shape of the thrombus, the maximum shear stress (138 dynes cm^{-2}) was located at the leading edge of the clot and was ~4-fold larger than the average clot shear stress (Fig. 4g).

Using the platelet-targeted thrombin sensor added to CTI-treated whole blood, the thrombin rich region was further analyzed at *trans*-scaffold ΔP = 0 and 23.4 mm Hg. The thrombin sensor provides a cumulative readout of local thrombin activity. Fluorescent line scans from the collagen interface (width = 0 microns) and across the clot into the blood flow (width = 45 microns) were averaged over the entire front-to-back length of the clot. In a diffusion-controlled transport process lacking transthrombus interstitial permeation (ΔP = 0 mm Hg), the thrombin concentration and boundary thickness were ~62% and ~59% larger, respectively, compared to that of clots formed with transthrombus permeation (ΔP = 23.4 mm Hg) (Fig. 5a and b). This drastic difference demonstrates

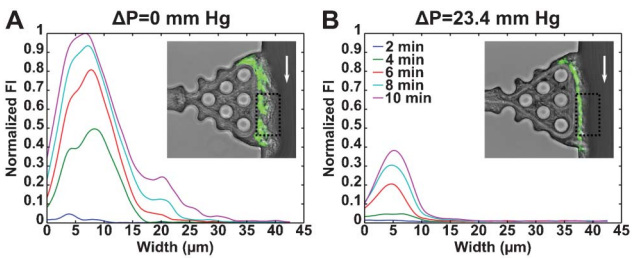

Fig. 5 Increasing transthrombus pressure gradients caused a reduction in thrombin. Average line scans of the thrombin boundary layer were taken every two minutes during clot formation on a collagen/TF surface. Whole blood anti-coagulated with CTI was perfused for 10 min and transthrombus pressure gradients were maintained at ΔP = 0 mm Hg (A) or ΔP = 23.4 mm Hg (B). The increased convection through the clot caused a reduction in the presence and velocity of thrombin towards the clot surface.

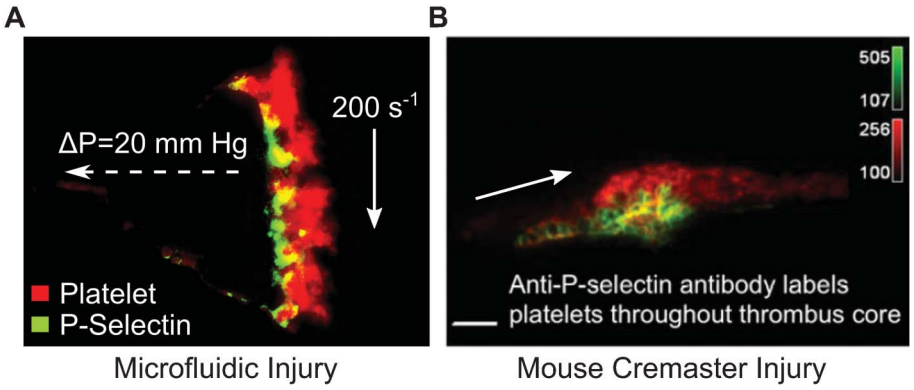

Fig. 6 Clots formed in the microfluidic injury model we present illustrate a remarkable correspondence to *in vivo* hierarchical clot architectures found in mice. Fluorescent P-selectin antibodies (green) were used to determine platelet α-granule release. Following 10 min of whole blood perfusion (200 s^{-1}) with a ΔP = 20 mm Hg, a distinct core of P-selectin positive platelets was covered by a shell of P-selectin negative platelets (red) in the microfluidic injury assay (A). The clot architecture of a thrombus in a mouse cremaster injury (ref. 21, with permission) demonstrates remarkable similarities (B). In both assays only the core or P-selectin positive platelets release their α-granules. This illustrates a level of activation that only the core region of the clot can reach during transthrombus permeation.

the important influence that transthrombus permeation has on soluble agonist localization. Since an inert protein the size of thrombin ($D_{Brownian} \sim 7 \times 10^{-7}$ cm^2 s^{-1}) would be expected to diffuse more than 100 microns in 4 min, the restricted ~15-micron thick region of thrombin activity in Fig. 5 indicates a combination of rapid inhibition by antithrombin, sequestration within fibrin, restricted diffusion by platelets, and/or platelet binding (*e.g.* platelet GPIbα). In addition to the thrombin studies, P-selectin positive platelets were also identified. Fig. 6 compares hierarchical clot architecture using human blood *in vitro* with a previously reported *in vivo* mouse laser injury model,[21] demonstrating a remarkable correspondence between these two independent approaches, namely the formation of a P-selectin-positive core and a surrounding P-selectin-negative shell. This is the first microfluidic device to recreate using human blood the core/shell architecture originally characterized in mouse blood vessels.

Pressure gradients affect thrombus composition and size

Using CTI-treated whole blood perfusion, the dynamics of clot composition, wall shear stress, and average clot height, in the presence (collagen/TF) or absence (collagen) of thrombin, were investigated at transthrombus pressure gradients of 20.8 mm Hg (Fig. 7a–d), 23.4 mm Hg (Fig. 7e–h), or 0 mm Hg (Fig. 7i–k). As the clot grew into the flow field, the wall shear stress increased under the constant flow rate conditions of the experiment. Since the average clot thickness (up to 50 μm) was small relative to the channel width (250 μm), the wall shear stress only increased modestly at a constant flow rate. The calculated clot wall shear stress was averaged in the middle 60% of the clot along the entire clot length.

A comparison of structures formed on collagen *versus* collagen/TF scaffolds at constant transthrombus pressure gradients revealed dramatically different structures. At ΔP = 20.8 mm Hg, the upstream portion of clots on the collagen remained larger than the trailing edge, whereas the trailing edge outgrew the upstream edge when whole blood was exposed to collagen/TF surfaces (Fig. 7a and b). In the case of ΔP = 23.4 mm Hg, the clots that developed on the collagen were relatively uniform along the length of the clot (Fig. 7e). At the same pressure, the incorporation of thrombin caused an initially larger upstream edge that eventually became uniform with the trailing edge following 10 min of perfusion (Fig. 7f). Noticeably, clots formed without transthrombus permeation (Fig. 7i) looked more similar to clots formed on collagen/TF surfaces at ΔP = 20.8 mm Hg, where the trailing edges protruded further into the flow. This phenomenon has been observed previously in a parallel channel microfluidic device at arterial wall shear stresses.[22]

Throughout all of the experiments, clot height decreased when the transthrombus pressure drop was increased. Interestingly, only an 11% increase in pressure drop (20.8 mm Hg to 23.4 mm Hg) resulted in large percentage reductions in final clot height for both collagen (27.9%, $p < 0.001$) and collagen/TF structures (20.2%, $p = 0.012$) (Fig. 7c and g). This trend continued when clots were formed without permeation. The final average clot height at ΔP = 0 mm Hg (TF/Collagen surface) was ~12 μm larger than clots exposed to transthrombus pressure gradients of 23.4 mm Hg (Fig. 7j). As previously discussed in Fig. 5, the thrombin boundary height was reduced with increasing ΔP (Fig. 7g and j). With the increases in clot heights came corresponding increases in wall shear stresses from an initial stress of 33.9 dynes cm^{-2} to 42.3 dynes cm^{-2} (platelet structures) or 46.9 dynes cm^{-2} (platelet/fibrin structures) (Fig. 7d and h).

Fluorescent dye transport allows thrombus permeability measurement

The designed microfluidic device not only allowed a side view analysis of thrombus development under transthrombus pressure gradients, but it was also a versatile tool for permeability measurements. In order to analyze the permeability measurements for platelet and platelet/fibrin clots formed under flow, the device was validated by comparing collagen permeability measurements to previous literature values. Measurements were made by injecting a fluorescent dye into the main channel under continuous flow and

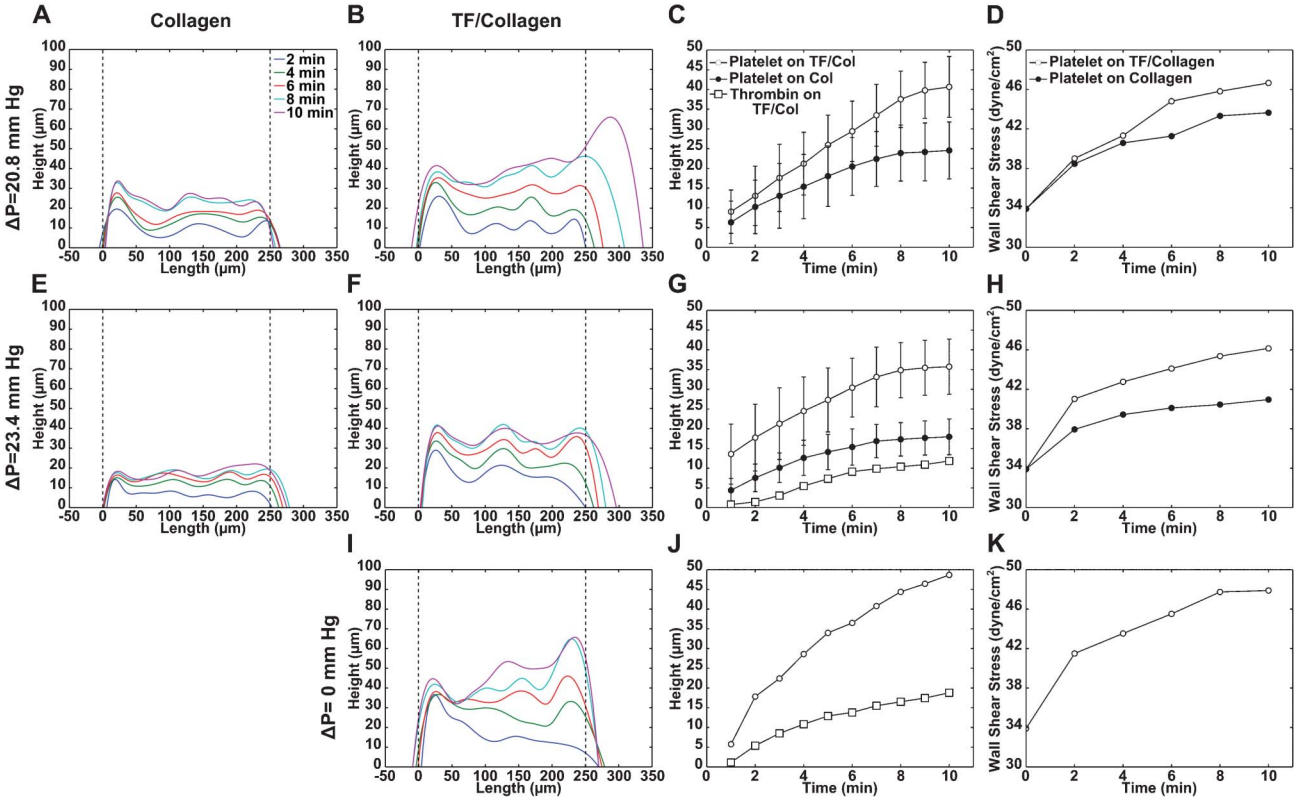

Fig. 7 Transthrombus pressure gradients effect dynamic measurements, such as clot structure, wall shear stress and height. Clots formed on collagen (± TF) with transthrombus pressure gradients of 20.8 mm Hg (A–D), 23.4 mm Hg (E–H), or 0 mm Hg (I–K) resulted in structural differences based on the pressure and the presence or absence of TF. Thrombus development on collagen without TF typically produced smaller clot heights and reduced wall shear stresses. A reductions in transthrombus pressure gradients resulted in increased thrombin and platelet deposition heights.

following the progression of the dye at the inlet and outlet of the collagen scaffold. From these curves, an average velocity was calculated by dividing the distance between measurements by the time between peak fluorescent intensities on both the inlet and outlet measurements. The calculated average velocities were then matched by minimizing the sum squared error between the predicted velocities through the structure in COMSOL. The measured permeability for the collagen scaffold was $1.98 \times 10^{-11} \pm 0.64 \times 10^{-11}$ cm^2. This value was within the range of collagen permeabilities (ref. 12: 8.9×10^{-11} cm^2; ref. 13: 1×10^{-11} cm^2) previously reported. This measurement was calculated for *trans*-scaffold pressure drops of 11.95 mm Hg, 14.15 mm Hg and 23.43 mm Hg.

With a validated measurement for the collagen scaffold, the next step was to measure the permeability of clots formed with and without thrombin. The addition of TF liposomes to the collagen and the substitution of CTI for PPACK allowed us to study platelet/fibrin clots. Using the same technique as previously discussed, measurements were made with collagen, and the concentration curves were validated by the COMSOL model (Fig. 8a and b). Without thrombin in the system, the platelet clot permeability was $5.45 \times 10^{-14} \pm 0.89 \times 10^{-14}$ cm^2 for ΔP = 20.70 mm Hg and 23.53 mm Hg (Fig. 8c). When thrombin was uninhibited, the time between peak dye intensities from the inlet to the outlet increased from 115 s to 280 s for the representative pulse curves. This increase resulted in a platelet/fibrin permeability of $2.71 \times 10^{-14} \pm 0.38 \times 10^{-14}$ cm^2 for ΔP = 20.76 mm Hg and 23.34 mm Hg (Fig. 8c). The 50% reduction in permeability ($p = 4.6 \times 10^{-4}$) can be seen by the relative increase in the time between peak dye intensities in the representative platelet ($\Delta t_{platelet}$ = 115 s) and platelet/fibrin ($\Delta t_{platelet/fibrin}$ = 280 s) clot curves. COMSOL was utilized to express these curves and the normalized dye concentration in the device at t = 3.33 min (Fig. 8d), t = 5.33 min (Fig. 8e), and t = 7.33 min (Fig. 8f) for the representative platelet/fibrin clot.

Discussion

The development of *in vitro* microfluidic assays and *in vivo* mouse injury models have provided many insights into thrombosis and hemostasis under physiological flow conditions.[7,23] While each assay has advantages, a challenge that still remains is the ability to study clot development and permeation at higher and lower physiological transthrombus pressure gradients. In the designed microfluidic device, clot development occurs under permeation, while being visualized from the side as in the mouse laser injury models. The advantage of incorporating these characteristics into a microfluidic model is the ability to control transthrombus pressure

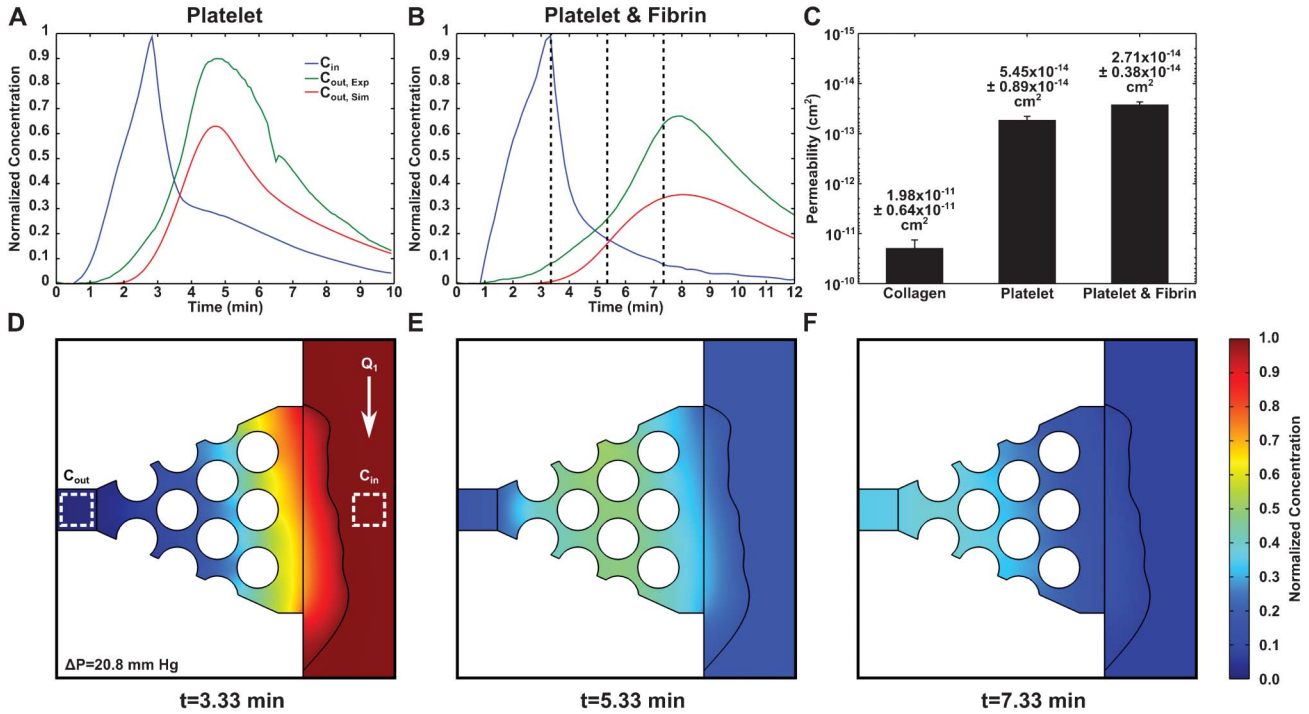

Fig. 8 Platelet and platelet/fibrin clot permeability was measured by pulsing fluorescent dyes. Following platelet deposition, whole blood flow was continuously switched to fluorescent dye injection. Dye fluorescence intensity was measured at the platelet (A) or platelet–fibrin (B) interface and the collagen exit to predict average fluid velocities across the structure. The permeability of the collagen scaffold, platelet clot, and platelet/fibrin clot were calculated using COMSOL to find the average velocity (C). Normalized dye fluorescence intensity was demonstrated in COMSOL at the time points indicated (D–F). The pulse was observed as it permeated through the collagen and platelet/fibrin structure.

gradients and wall shear stresses. This is the first reported device that facilitates the independent control of both of these important regulators of clot development at physiological vessel conditions.

Studies of interstitial flow and its importance in angiogenesis and other cellular environments have steadily increased over the last decade. Incorporating controllable pressure gradients and wall shear stress in a model of angiogenesis may provide a more realistic *in vitro* representation of the process as it pertains to human physiology. In the case for thrombosis and hemostasis, minimal changes of transthrombus pressure gradients revealed a significant change in clot size and structure. The increase in transthrombus permeation caused by an increase in pressure gradients resulted in decreased clot height. The diffusivity of agonists such as thrombin, ADP, and TXA_2 play an important role in these observations. In a thrombin deficient scenario, platelet aggregation is primarily achieved by the release of ADP and TXA_2 after the initial adhesion to the exposed collagen. The diffusivity of these molecules is much faster than thrombin and as a result, are more easily affected by transthrombus permeation.[24] When thrombin is present, the reduction in clot size is still noticeable at increased pressure gradients, but slightly reduced compared to the previous scenario. This interpretation was supported by the reduction in thrombin boundary height in clots formed in the presence of transthrombus permeation. Without pressure gradients, the thrombin was allowed to diffuse further towards the surface of the clot. This suggests that ADP or TXA_2 would easily reach the clot surface under these conditions, but would be convected quickly away under permeation.[25] Studying the dynamics of thrombosis and hemostasis under transthrombus permeation has allowed for a more thorough investigation of the platelets' response to the physical and biological stimuli present in physiology.

While clot structure and size were affected by pressure gradients, the permeability of platelet and platelet/fibrin thrombus formed under these conditions remained constant. Permeability measurements in microfluidic devices are not novel,[26] but the measurement of thrombus permeability under flow certainly is. Previous measurements have fallen short in their attempt to predict physiological clot permeability due to the omission of clot structure and composition only observed under flow.[27] In this device, these critical features were preserved and clot permeability measurements were obtained in the presence and absence of thrombin. The permeability observed in these measurements compares closely to previous measurements made in rabbit endothelium,[28] suggesting that these clots may be a rapidly developing replacement tissue for the denuded endothelium. This would allow the necessary wound healing molecules and cells access to the site of injury, while maintaining vessel hemostasis. Incorporation of tissue factor molecules allowed clots to quickly intertwine fibrin into their structure and resulted in a significant reduction in

permeability as compared to thrombin/fibrin deficient clots. This is important because clots formed in low tissue factor areas, such as joints, may rely solely on thrombin production from the intrinsic pathway.[29] The reduction in their permeability allows increased access to the site of injury. The increase in access may be correlated to cases of joint bleeding in hemophiliacs where thrombin production *via* the intrinsic pathway is limited.[30] The device implemented in these studies has proved to be a great way to measure permeability and the role of pressure gradients on clot development. Moving forward, this device would provide valuable data to the fields of angiogenesis and thrombosis, where interstitial permeation plays a critical role in the functionality of the assay.

Conclusions

While investigating thrombus development on a collagen or collagen/TF scaffold we were able to conclude that small reductions in transthrombus pressure drop caused significant increases in average clot height. This observation was also observed during a study of agonist localization. In the presence of clot permeation the thrombin boundary height and intensity were substantially reduced compared to a scenario where diffusion dominated clot transport. Additionally, measurements for collagen permeability were validated with previous literature values and clot permeabilities were easily measured under continuous flow conditions at varying pressure drops. This device provides a novel system that is translatable to studies requiring independent control of physiological *trans*-scaffold pressure gradients and/or wall shear stresses.

Acknowledgements

This study was supported by NIH R01 HL103419 (S. L. D.).

References

1 K. S. Sakariassen, P. A. Bolhuis and J. J. Sixma, *Nature*, 1979, **279**, 636–638.
2 V. T. Turitto and H. R. Baumgartner, *Microvasc. Res.*, 1979, **17**, 38–54.
3 H. H. Lipowsky, in *Flow-Dependent Regulation of Vascular Function*, ed. J. A. Bevan, G. Kaley and G. M. Rubanyi, Oxford University Press, New York, 1995, ch. 2, pp. 28–45.
4 C. H. Heldin, K. Rubin, K. Pietras and A. Ostman, *Nat. Rev. Cancer*, 2004, **4**, 806–813.
5 D. Fukumura and R. K. Jain, *Microvasc. Res.*, 2007, **74**, 72–84.
6 V. Vickerman, J. Blundo, S. Chung and R. Kamm, *Lab Chip*, 2008, **8**, 1468–1477.
7 K. B. Neeves, S. F. Maloney, K. P. Fong, A. A. Schmaier, M. L. Kahn, L. F. Brass and S. L. Diamond, *J. Thromb. Haemostasis*, 2008, **6**, 2193–2201.
8 K. B. Neeves and S. L. Diamond, *Lab Chip*, 2008, **8**, 701–709.
9 D. C. Duffy, J. C. McDonald, O. J. A. Schueller and G. M. Whitesides, *Anal. Chem.*, 1998, **70**, 4974–4984.
10 S. A. Smith and J. H. Morrissey, *J. Thromb. Haemostasis*, 2004, **2**, 1155–1162.
11 T. V. Colace, J. Jobson and S. L. Diamond, *Bioconjugate Chem.*, 2011, **22**, 2104–2109.
12 R. Sudo, S. Chung, I. K. Zervantonakis, V. Vickerman, Y. Toshimitsu, L. G. Griffith and R. D. Kamm, *FASEB J.*, 2009, **23**, 2155–2164.
13 S. Ramanujan, A. Pluen, T. D. McKee, E. B. Brown, Y. Boucher and R. K. Jain, *Biophys. J.*, 2002, **83**, 1650–1660.
14 S. E. Parazynski, A. R. Hargens, B. Tucker, M. Aratow, J. Styf and A. Crenshaw, *J. Appl. Physiol.*, 1991, **71**, 2469–2475.
15 H. Wiig, *Crit. Rev. Biomed. Eng.*, 1990, **18**, 27–54.
16 J. D. Welsh, T. V. Colace, R. W. Muthard, T. J. Stalker, L. F. Brass and S. L. Diamond, *J. Thromb. Haemostasis*, 2012, **10**, 2344–2353.
17 R. I. Litvinov, O. V. Gorkun, D. K. Galanakis, S. Yakovlev, L. Medved, H. Shuman and J. W. Weisel, *Blood*, 2007, **109**, 130–138.
18 B. Kudryk, A. Rohoza, M. Ahadi, J. Chin and M. E. Wiebe, *Mol. Immunol.*, 1984, **21**, 89–94.
19 R. W. Muthard and S. L. Diamond, *Arterioscler., Thromb., Vasc. Biol.*, 2012, **32**, 2938–2945.
20 R. E. Wells and E. W. Merrill, *J. Clin. Invest.*, 1962, **41**, 1591–1598.
21 T. J. Stalker, E. A. Traxler, J. Wu, K. M. Wannemacher, S. L. Cermignano, R. Voronov, S. L. Diamond and L. F. Brass, *Blood*, 2013, **121**, 1875–1885.
22 T. V. Colace, R. W. Muthard and S. L. Diamond, *Arterioscler., Thromb., Vasc. Biol.*, 2012, **32**, 1466–1476.
23 S. Falati, P. Gross, G. Merrill-Skoloff, B. C. Furie and B. Furie, *Nat. Med.*, 2002, **8**, 1175–1180.
24 J. A. Hubbell and L. V. McIntire, *Biophys. J.*, 1986, **50**, 937–945.
25 M. H. Flamm, T. V. Colace, M. S. Chatterjee, H. Jing, S. Zhou, D. Jaeger, L. F. Brass, T. Sinno and S. L. Diamond, *Blood*, 2012, **120**, 190–198.
26 E. W. K. Young, M. W. L. Watson, S. Srigunapalan, A. R. Wheeler and C. A. Simmons, *Anal. Chem.*, 2010, **82**, 808–816.
27 J. P. Collet, G. Montalescot, C. Lesty, J. Soria, Z. Mishal, D. Thomasand and C. Soria, *Arterioscler., Thromb., Vasc. Biol.*, 2001, **21**, 142–148.
28 A. Tedgui and M. J. Lever, *Am. J. Physiol.*, 1984, **247**, H784–791.
29 T. A. Drake, J. H. Morrissey and T. S. Edgington, *Am. J. Pathol.*, 1989, **134**, 1087–1097.
30 M. J. Manco-Johnson, T. C. Abshire, A. D. Shapiro, B. Riske, M. R. Hacker, R. Kilcoyne, J. D. Ingram, M. L. Manco-Johnson, S. Funk, L. Jacobson, L. A. Valentino, W. K. Hoots, G. R. Buchanan, D. DiMichele, M. Recht, D. Brown, C. Leissinger, S. Bleak, A. Cohen, P. Mathew, A. Matsunaga, D. Medeiros, D. Nugent, G. A. Thomas, A. A. Thompson, K. McRedmond, J. M. Soucie, H. Austin and B. L. Evatt, *N. Engl. J. Med.*, 2007, **357**, 535–544.